

SIMPLIFIED J-INTEGRAL ESTIMATION FOR A FLAT PLATE WITH A SURFACE CRACK UNDER MULTIAXIAL LOADING

Takuya Ogawa¹, Shuichi Yoshida², Masao Itatani³,
Takahiro Hayashi⁴, Chihiro Narazaki⁵, Toshiyuki Saito⁶

¹ Manager, Toshiba Energy Systems & Solutions Corporation, Yokohama, Japan
(takuya4.ogawa@toshiba.co.jp)

² Toshiba Energy Systems & Solutions Corporation, Yokohama, Japan (shuichi5.yoshida@toshiba.co.jp)

³ Toshiba Energy Systems & Solutions Corporation, Yokohama, Japan (masao.itatani@toshiba.co.jp)

⁴ Fellow, Toshiba Energy Systems & Solutions Corporation, Yokohama, Japan
(takahiro7.hayashi@toshiba.co.jp)

⁵ Specialist, Toshiba Energy Systems & Solutions Corporation, Yokohama, Japan
(chihiro.narazaki@toshiba.co.jp)

⁶ Toshiba Energy Systems & Solutions Corporation, Yokohama, Japan (toshi.saito@toshiba.co.jp)

ABSTRACT

Service life management is a key issue for improving the safety of light water reactors. When a crack is detected in a nuclear component, the structural integrity of the component must be evaluated. Appendix E-9 of “*Rules on Fitness-for-Service for Nuclear Power Plants*” of the Japan Society of Mechanical Engineers Code (JSME FFS Code) provides a fracture assessment methodology based on elastic–plastic fracture mechanics (EPFM). The fracture mechanics parameter J-integral is commonly used in the elastic–plastic field. Although the reference stress method is well-known as a simple solution for estimating the J-integral without finite element analysis (FEA), most of the simple solutions for a flat plate are only applicable under uniaxial loading conditions. This study investigated the effect of multiaxial loading on the J-integral and proposes a simple method for estimating the J-integral under multiaxial loading. The J-integral of a flat plate with a semi-elliptical surface crack was examined by FEA under various multiaxial loading conditions. The ratio of the stress perpendicular to the crack plane (σ_1) to the stress parallel to the crack plane (σ_2) was denoted as α ($= \sigma_2/\sigma_1$), and six values of α were considered: 0 (uniaxial), 0.5, 0.8, 1.0, 1.5, and 2.0. The FEA results revealed that the multiaxial loading conditions affected the J-integral compared to that under uniaxial conditions when organizing based on the stress perpendicular to the crack plane. This study proposes a multiaxial correction factor for the yield stress in the stress–strain relationship in order to estimate the J-integral under multiaxial loading conditions by utilizing the existing reference stress method under uniaxial loading conditions. A comparison of the FEA results and the results from the simple estimation method proposed in this study shows that the proposed method generally provides a good estimation of the J-integral under multiaxial loading conditions with reasonable accuracy for various α values.

INTRODUCTION

In the nuclear power industry, stress corrosion cracking (SCC) is an important issue for improving the safety of light water reactors (see Bamford et al. 2003, Matsunaga et al. 2003, Aoki et al. 2005, Bjurman et al. 2017 and NRC 2017). When a crack is detected in a nuclear component, the structural integrity of the component must be evaluated. “*Rules on Fitness-for-Service for Nuclear Power Plants*” of the Japan Society of Mechanical Engineers Code (JSME FFS Code) and Section XI of the ASME Boiler and Pressure Vessel Code (Sec. XI of the ASME Code) provide flaw evaluation methodologies, including fracture assessment methodologies for components with a crack. Specifically, Appendix E-9 of the JSME FFS Code and Nonmandatory Appendix K of Sec. XI of the ASME Code provide a fracture assessment methodology

based on elastic–plastic fracture mechanics (EPFM), which requires the calculation of the J-integral due to the applied loads accounting for elastic–plastic behavior of the stress–strain relationship of the material. Although finite element analysis (FEA) is generally needed to obtain the J-integral due to applied loads, the reference stress method is well-known as a simple solution for estimating the J-integral without FEA.

The authors recently reported that a fracture assessment methodology based on the EPFM can be applied to the dissimilar metal weld (DMW) of reactor pressure vessel (RPV) bottom head components of a boiling water reactor (BWR) consisting of Ni-base alloy weld metal and low alloy steel (LAS) (see Hayashi et al. 2021). ASME Code Case N-749 provides alternative acceptance criteria based on the EPFM for flaws in ferritic components when the service temperature of the components is in the upper shelf temperature range (Gustin et al. 2012). Here, since the DMW of the RPV bottom head components has a complex geometry, it is modeled into a simple, flat plate geometry, as recommended in Appendix E-13 of the JSME FFS Code. Although the loads applied to the DMW described here are not always uniaxial, most of the reference stress solutions for a flat plate with a surface crack are only applicable to uniaxial loading conditions. This study investigated the effect of multiaxial loading conditions, such as biaxial and triaxial loading, on the J-integral.

EFFECT OF BIAXIAL LOADING ON J-INTEGRAL

FE Analysis Conditions

The effect of biaxial loading conditions on the J-integral was investigated by FEA. The flat plate model was defined as having a thickness of 178 mm and a plate width of 1780 mm. The surface crack was modeled as a semi-elliptical shape with a depth of 10 mm and a length of 60 mm. The commercial FEA code “ABAQUS” was used, and the element type was the hexahedral C3D8. Considering symmetry, a half model was adopted, and the symmetrical boundary conditions were defined on the symmetry planes except for the crack plane. Additionally, the node constraints were defined in the thickness direction and the plate width direction to prevent rigid body motion. The nodes were arranged along the front edge of the surface crack, and element subdivision was conducted. The analysis model is shown in Figure 1.

As can be seen in Figure 2, biaxial loading is defined on the analysis model as stress perpendicular to the crack plane (σ_1) and stress parallel to the crack plane (σ_2). In this study, the ratio of σ_1 to σ_2 was denoted as α ($= \sigma_2/\sigma_1$), and six values of α were considered: $\alpha = 0, 0.5, 0.8, 1.0, 1.5,$ and 2.0 . Note that $\alpha = 0$ corresponds to uniaxial loading conditions, and $\alpha = 1.0$ corresponds to equibiaxial conditions where the stresses perpendicular and parallel to the crack plane are equal. When substituting a flat plate for the cylindrical part of a pressure vessel subjected to internal pressure, the theoretical solution indicates that the axial stress is half of the circumferential (hoop) stress. In the case of an axial crack in a pressure vessel, the stress perpendicular to the crack plane corresponds to the circumferential (hoop) stress, and the stress parallel to the crack plane corresponds to the axial stress, resulting in a ratio of $\alpha = 0.5$. Similarly, for a circumferential crack in a pressure vessel, $\alpha = 2.0$ is assumed.

Material properties with a Young’s modulus of 191000 MPa and a Poisson’s ratio of 0.3 were used for the FEA. The stress–strain relationship was approximated using the Ramberg–Osgood model, based on the tensile test results at room temperature of low alloy steel SFVQ1A used in a RPV (Hayashi et al. 2021). The stress–strain relationship is shown in Equation 1. Figure 3 shows the relationship between the stress and plastic strain obtained by Equation 1.

$$(\varepsilon/\varepsilon_y) = (\sigma/\sigma_y) + C(\sigma/\sigma_y)^n \quad (1)$$

where ε is the strain, σ is the stress, σ_y is the yield stress (455 MPa), ε_y is the yield strain (σ_y/E , $E = 191000$ MPa), and C and n are the fitting parameters ($C = 2.817$, $n = 7.878$).

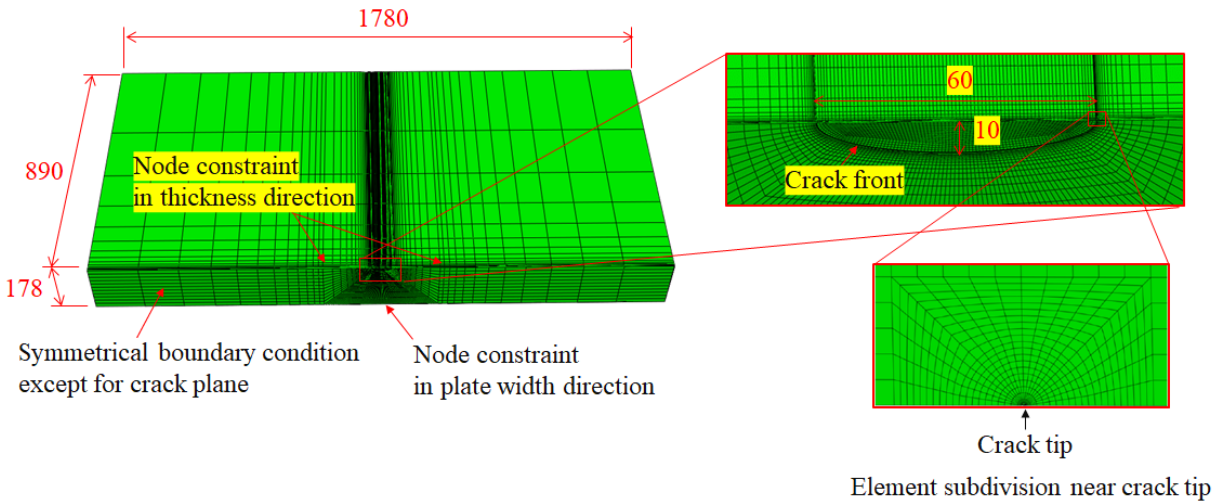


Figure 1. Analysis model for a flat plate with a surface crack.

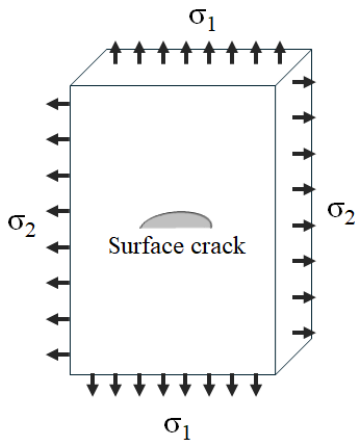


Figure 2. Biaxial loading defined on the flat plate model.

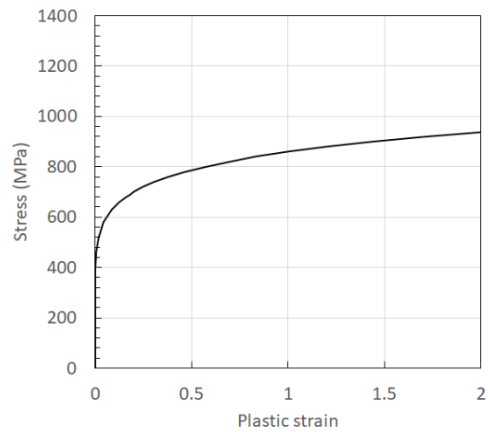
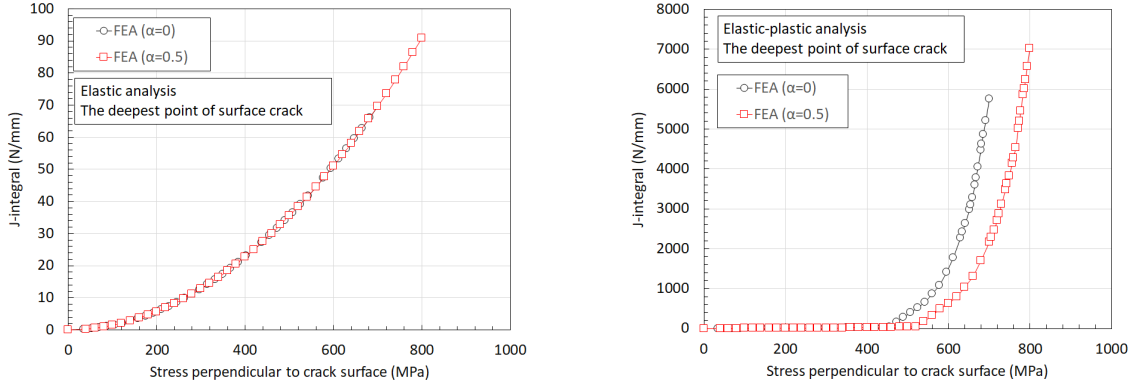


Figure 3. Stress-plastic strain relationship.

Comparison of Elastic Analysis and Elastic-Plastic Analysis

Prior to examining the results for various biaxial loading conditions, a comparison was made between the elastic analysis and elastic-plastic analysis under two conditions, $\alpha = 0$ and 0.5 , as shown in Figure 4. The J-integral at the deepest point of the surface crack was evaluated in each analysis. Figures 4(a) and 4(b) respectively show the J-integral at the deepest point of the crack organized by the stress perpendicular to the crack plane in the elastic analysis and elastic-plastic analysis. In the case of the elastic analysis, the J-integrals for $\alpha = 0$ and 0.5 match well, suggesting that when deriving linear elastic fracture mechanics parameters such as stress intensity factor, it is sufficient to consider only the stress perpendicular to the crack plane. On the other hand, in the elastic-plastic analysis, there is a difference in the J-integrals between $\alpha = 0$ and 0.5 , which indicates that multiaxial loading has an effect on the J-integral in the elastic-plastic stress field.



(a) Elastic analysis

(b) Elastic-plastic analysis

Figure 4. Comparison between elastic analysis and elastic-plastic analysis under $\alpha = 0$ and 0.5.

Elastic-Plastic Analysis Results for Various Biaxial Loading Conditions

The results of the elastic-plastic analyses confirmed the macroscopic deformation behavior for the representative conditions of $\alpha = 0, 0.5$, and 1.0. Figure 5 shows the comparison results between the undeformed and deformed shapes of the flat plate. For $\alpha = 0$ (uniaxial), deformation occurs in the loading direction (perpendicular to the crack plane), and a contraction corresponding to a plastic Poisson's ratio of 0.5 is observed in the direction parallel to the crack plane. For $\alpha = 0.5$, the contraction in the direction parallel to the crack plane is offset by the deformation due to the load in the direction parallel to the crack plane, and macroscopically, only the deformation perpendicular to the crack plane is recognized. For $\alpha = 1.0$ (equibiaxial), equivalent deformation occurs in the perpendicular and parallel directions to the crack plane. From these macroscopic deformation behaviors, no peculiar deformation is observed.

In the FEA, the elastic-plastic J-integral was calculated by the contour integral method. Since it is generally known that using this method results in a path dependency for the J-integral, the path dependency of the J-integral at the deepest point of the surface crack for $\alpha = 0$ (uniaxial) was confirmed. The relationship between the integration path number and the J-integral is shown in Figure 6. The elastic-plastic J-integral for integration paths 1 to 20 is plotted in the figure. Although a path dependency was observed between integration paths 1 to 5, no distinct path dependency is observed between integration paths 6 to 20, and it converges to almost a constant value. Therefore, in this study, the average value for integration paths 16 to 20 was used to evaluate the elastic-plastic J-integral.

The results of the elastic-plastic J-integral analysis for $\alpha = 0, 0.5, 0.8, 1.0, 1.5$, and 2.0 revealed the relationship between the J-integral and the stress perpendicular to the crack plane, as shown in Figure 7. Focusing on the J-integral for $\alpha = 0$ (uniaxial), it can be seen that when the horizontal axis exceeds 455 MPa, the increase in the J-integral becomes significant along with the increase in the stress. Since 455 MPa corresponds to the yield stress used in the FEA, it was found that the plastic component in the J-integral increased. For $\alpha = 1.0$ (equibiaxial), the J-integral was almost the same as that for $\alpha = 0$ (uniaxial). For $\alpha = 0.5$ and 0.8, the increase in the plastic component in the J-integral shifted to the right on the horizontal axis, and the J-integral after the increase in the plastic component was smaller than that in the uniaxial case. On the other hand, for $\alpha = 1.5$ and 2.0, the increase in the plastic component in the J-integral shifted significantly to the left on the horizontal axis, and the J-integral after the increase in the plastic component was much larger than that in the uniaxial case. From these analysis results, it can be seen that if only the stress component perpendicular to the crack plane is considered, when the actual stress multiaxiality corresponds to $\alpha = 0.5$ or 0.8, the J-integral will be overestimated, and when it corresponds to $\alpha = 1.5$ or 2.0, the J-integral will be underestimated. Figure 8 organizes the analysis results of the J-integral by the von Mises

stress. Regardless of the difference in α , the von Mises stress at which the plastic component of the J-integral manifests was consistent at 455 MPa. However, the value of the J-integral after the increase in the plastic component varied depending on α . The above trends were observed at both the deepest point and the surface point of the surface crack.

To further discuss the effects of biaxial loading conditions on the J-integral, the stress distribution near the crack tip at the deepest point of the crack was evaluated. Figure 9 shows a comparison of the stress distributions near the crack tip for various α values when the J-integral at the deepest point of the crack was approximately 1500–2500 N/mm. Although differences were observed in the stresses perpendicular and parallel to the crack plane depending on α , they matched well when organized by the von Mises stress. This suggests that the biaxial loading conditions influence the stress distribution near the crack tip, thus affecting the J-integral. Furthermore, Figure 10 compares the stress distribution near the crack tip when the stress perpendicular to the crack plane was 595 MPa for $\alpha = 0$ (uniaxial) and 589 MPa for $\alpha = 1.5$. The J-integral at the deepest point of the crack was 1410 N/mm for $\alpha = 0$ and 6078 N/mm for $\alpha = 1.5$, indicating a significant difference in the J-integral. As shown in Figure 10, differences were also observed in the von Mises stress distribution.

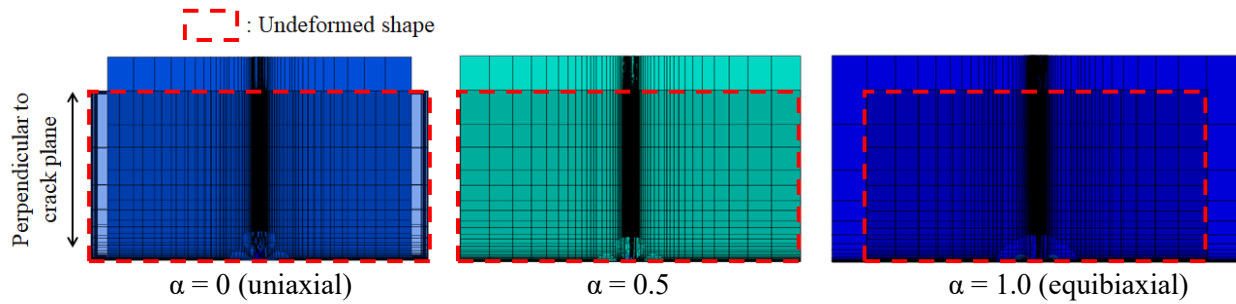


Figure 5. Comparison between the undeformed and deformed shapes of the flat plate.

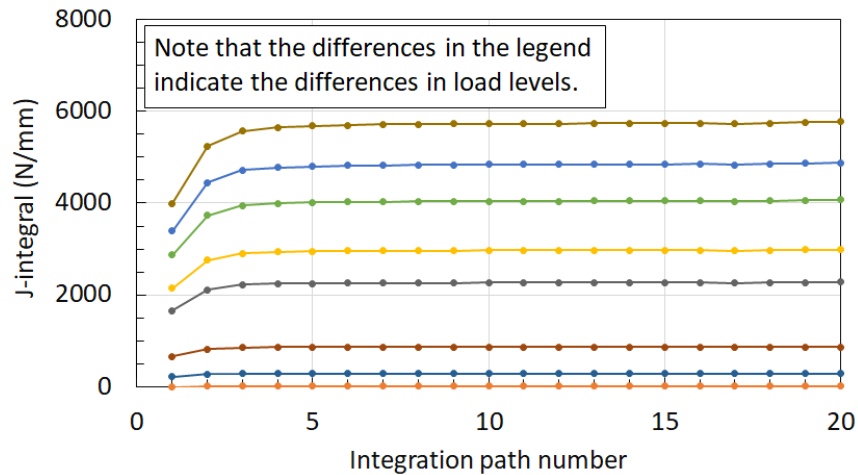


Figure 6. Example of the path dependency of the J-integral.

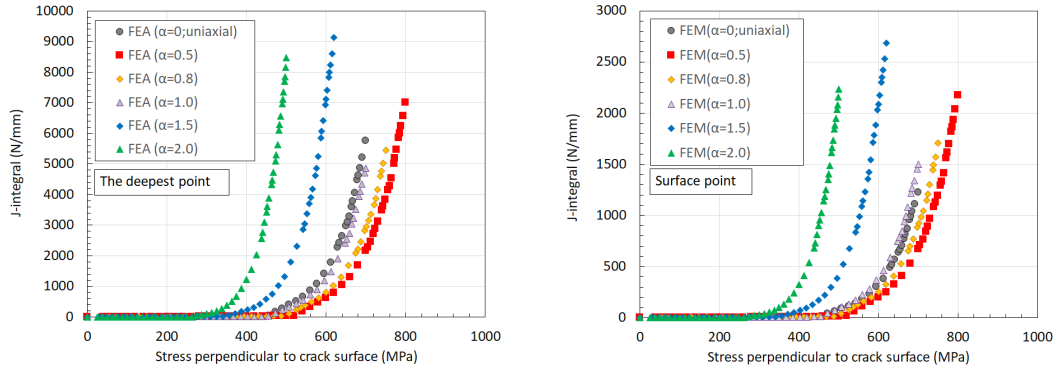


Figure 7. Relationship between the J-integral and the stress perpendicular to the crack plane. (Left: deepest point, Right: surface point)

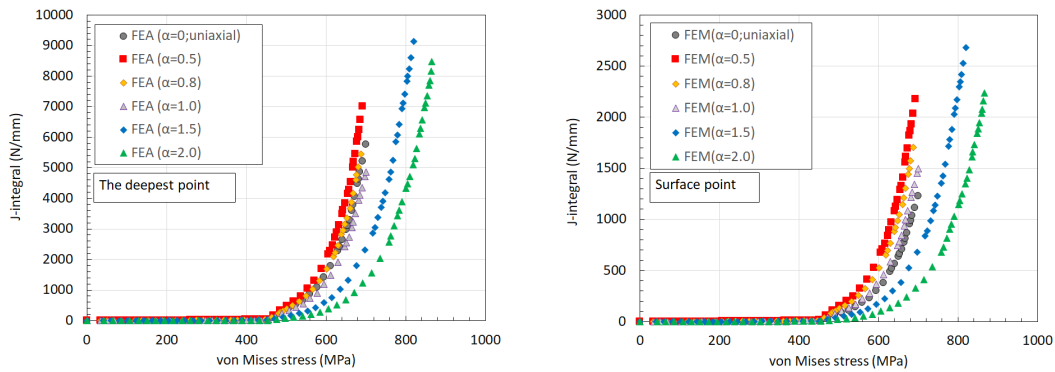


Figure 8. Relationship between the J-integral and the von Mises stress. (Left: deepest point, Right: surface point)

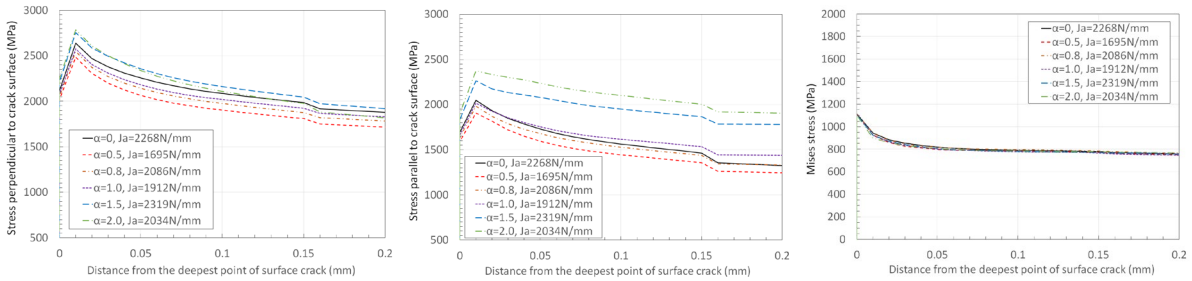


Figure 9. Stress distributions near the crack tip for approximately 1500–2500 N/mm.

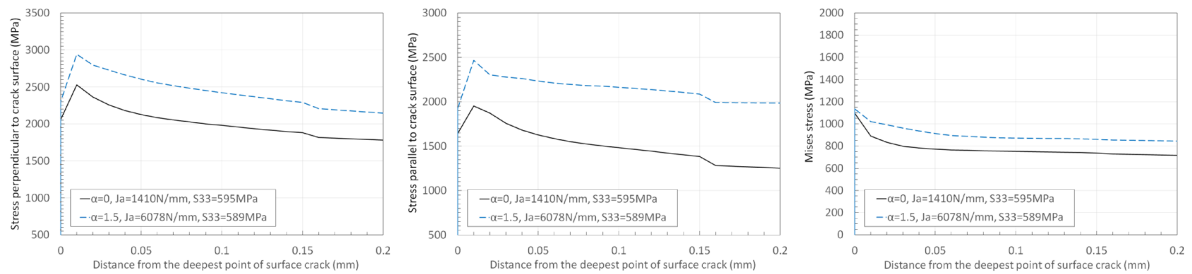


Figure 10. Stress distributions near the crack tip for almost the same stress perpendicular to the crack plane.

PROPOSAL OF SIMPLIFIED ESTIMATION SOLUTION FOR J-INTEGRAL

Reference Stress Method under Uniaxial Loading Conditions

Several reference stress solutions have been reported for a flat plate with a surface crack subjected to a uniaxial tensile load, as shown in Figure 11 (Lei 2004, Sattari-Far 1994, Miura et al. 2000). The reference stress solution adopted in this study was modified by Lei from the equation of Goodall and Webster (Lei 2004) given by Equations 2 through 5. It was reported that this solution provided good estimations of the J-integral values (Takanashi et al. 2023).

$$\sigma_{ref} = \frac{\sigma_m}{F_t} \quad (2)$$

$$F_t = \frac{d_1}{\gamma + \sqrt{\gamma^2 + d_1}} \quad (3)$$

$$d_1 = (1 - \gamma^2) + 2\gamma(\varphi - \gamma) \quad (4)$$

$$\gamma = \varphi\omega, \quad \varphi = \frac{a}{t}, \quad \omega = \frac{c}{W} \quad (5)$$

where σ_m is the membrane stress ($= P/(2Wt)$), a is the crack depth, c is half the crack length, t is the plate thickness, W is half the plate width. The J-integrals were estimated from the reference stress using Equations 6 and 7 without the small-scale yielding correction. Note that the stress intensity factors (K) were estimated by the Raju and Newman solution (Newman et al. 1981).

$$J_e = (1 - \nu^2) \frac{K^2}{E} \quad (6)$$

$$J = \frac{E\epsilon_{ref}}{\sigma_{ref}} J_e \quad (7)$$

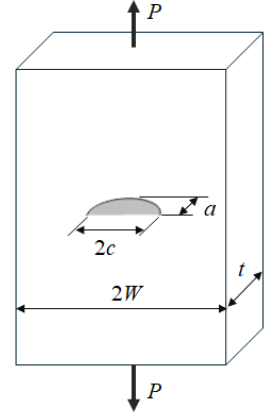


Figure 11. Geometry of a flat plate with a surface crack.

Proposal of Multiaxial Correction Factor

The FEA results described above suggest that the stress distribution near the crack tip varies due to biaxial loading, thereby affecting the J-integral. It was shown that the von Mises stress distribution near the crack tip matches well when the J-integral values are similar. On the other hand, most of the existing reference stress solutions are only applicable under uniaxial loading conditions. In this study, a multiaxial correction factor was investigated to obtain a practical estimation of the J-integral under biaxial loading using the reference stress solution for uniaxial loading conditions.

As is generally known, von Mises stress is calculated from three principal stresses σ_1 , σ_2 , and σ_3 using Equation 8. Here, for biaxial loading, σ_2 is equal to $\alpha\sigma_1$, and σ_3 is equal to zero. Solving Equation 8 with respect to σ_1 leads to Equation 9. This coefficient is defined as a multiaxial correction factor γ , as shown in Equation 10. Figure 12 shows the relationship between α and γ . When α is greater than 0 and less than 1.0, γ is greater than 1.0. When α is greater than 1.0, γ is less than 1.0. The multiaxial correction factor γ was applied for correcting the yield stress of the stress–strain relationship shown in Equation 1. The corrected stress–strain relationship for estimating the J-integral under biaxial loading is shown in Equation 11. Figure 13 shows the corrected stress–strain relationships for $\alpha = 0, 0.5, 0.8, 1.0, 1.5,$ and 2.0 .

$$\sigma_{mises} = \sqrt{\frac{(\sigma_1 - \sigma_2)^2 + (\sigma_1 - \sigma_3)^2 + (\sigma_2 - \sigma_3)^2}{2}} \quad (8)$$

$$\sigma_1 = \frac{\sigma_{mises}}{\sqrt{\alpha^2 - \alpha + 1}} \tag{9}$$

$$\gamma = \frac{1}{\sqrt{\alpha^2 - \alpha + 1}} \tag{10}$$

$$(\varepsilon/\varepsilon_y) = (\sigma/(\gamma\sigma_y)) + C(\sigma/(\gamma\sigma_y))^n \tag{11}$$

where ε_y is the yield strain ($(\gamma\sigma_y)/E$, $E = 191000$ MPa), and C and n are the fitting parameters ($C = 2.817$, $n = 7.878$).

Estimation of the J-integral was performed using the reference stress solution with the corrected stress–strain relationship and then compared with the FEA results. Here, only the stress perpendicular to the crack plane was considered. Figure 14 compares the reference stress solution with the FEA results when the horizontal axis is the stress perpendicular to the crack plane. It can be seen that the changes in the J-integral due to biaxial loading (a rightward shift on the horizontal axis for $\alpha = 0.5$ and 0.8 , and a leftward shift for $\alpha = 1.5$ and 2.0) are generally well estimated. In some cases, although there are small discrepancies between the reference stress solution and the FEA results, they are comparable to the discrepancies observed under uniaxial loading conditions ($\alpha = 0$). It has been shown that a practical estimation of the J-integral under biaxial loading can be obtained by using the stress–strain relationship corrected by the multiaxial correction factor and the reference stress solution for uniaxial loading. Additionally, when α is between 0 and 1.0, it has been shown that the J-integral can be conservatively estimated by considering only the stress perpendicular to the crack plane and using the reference stress solution for uniaxial loading.

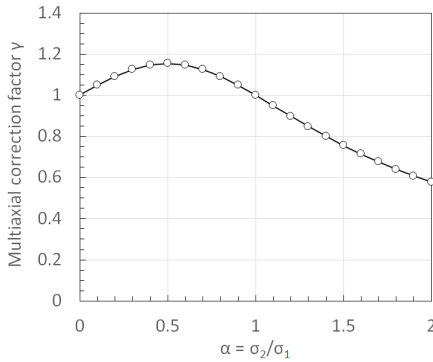


Figure 12. Relationship between α and γ .

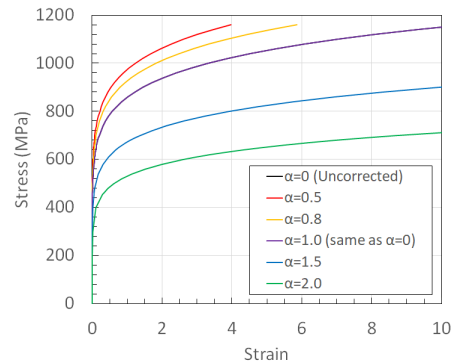


Figure 13. Corrected stress–strain relationships.

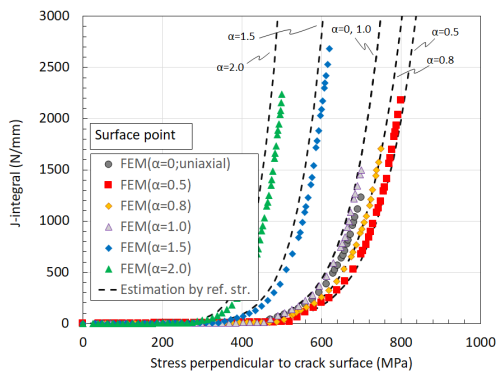
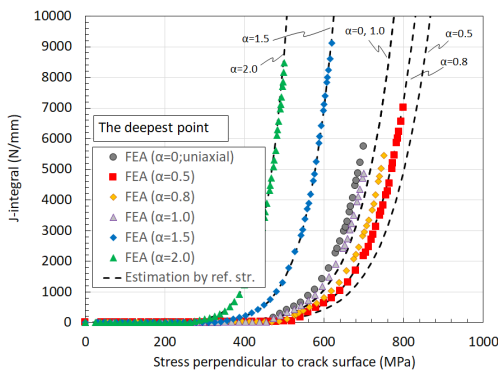


Figure 14. Comparison of the J-integral estimation between reference stress solution and FEA results.
 (Left: deepest point, Right: surface point)

J-INTEGRAL ESTIMATION UNDER TRIAXIAL LOADING CONDITIONS

This section discusses the extension of the multiaxial correction factor to triaxial loading. The shape and dimensions of the evaluation model remain the same as in Figure 1, and in addition to the biaxial loading of the flat plate shown in Figure 2, which is stress perpendicular to the crack plane (σ_1) and stress parallel to the crack plane (σ_2), the stress in the thickness direction (σ_3) of the flat plate is defined. As an index representing the stress multiaxiality, in addition to the ratio α of σ_1 to σ_2 , β as the ratio of σ_1 to σ_3 ($\beta = \sigma_3/\sigma_1$) is also defined. In Equation 8, σ_2 is equal to $\alpha\sigma_1$ and σ_3 is equal to $\beta\sigma_1$ for triaxial loading. Therefore, the multiaxial correction factor γ for triaxial loading is obtained by solving Equation 8 with respect to σ_1 , as shown in Equation 12.

$$\gamma = \frac{1}{\sqrt{\alpha^2 + \beta^2 - \alpha\beta - \alpha - \beta + 1}} \quad (12)$$

Two cases were set for the triaxial loading conditions: $\alpha = 0.5$, $\beta = 0.2$, and $\alpha = 2.0$, $\beta = 0.2$. The J-integral under triaxial loading was calculated using FEA, and the results were compared with the reference stress solution using the multiaxial correction factor γ and the stress perpendicular to the crack plane, as shown in Figure 15. It has been shown that a practical estimation can be obtained for the J-integral under triaxial loading.

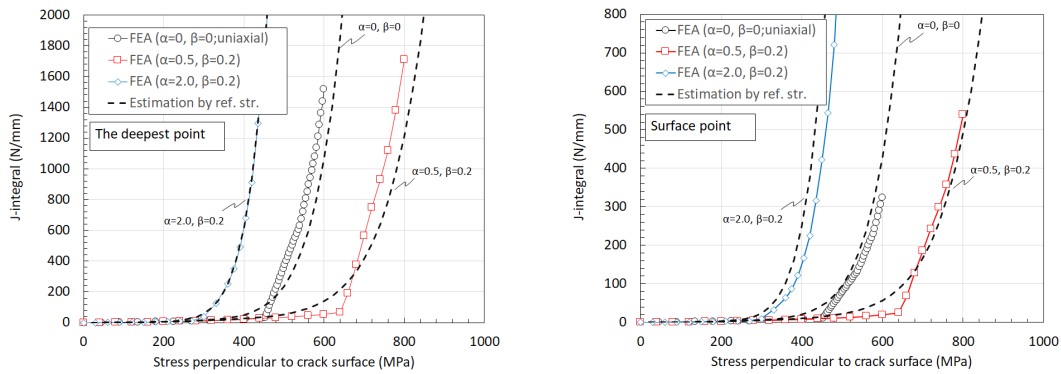


Figure 15. Comparison of the J-integral estimation by reference stress solution with FEA results under triaxial loading. (Left: deepest point, Right: surface point)

CONCLUSION

This study investigated the effect of multiaxial loading conditions, such as biaxial and triaxial loading, on the J-integral. A simple estimation method was proposed for the J-integral under multiaxial loading. The conclusions obtained are summarized below.

- (1) The elastic–plastic analysis results confirmed the effect of biaxial loading on the J-integral. It was considered that the biaxial loading influences the stress distribution near the crack tip, thus affecting the J-integral. When the J-integrals were almost the same values, the von Mises stress distribution near the crack tip matched well.
- (2) If only the stress component perpendicular to the crack plane is considered, it was found that the J-integral will be overestimated when the actual stress multiaxiality corresponds to $\alpha = 0.5$ or 0.8 , while the J-integral will be underestimated when the actual stress multiaxiality corresponds to $\alpha = 1.5$ or 2.0 .
- (3) A multiaxial correction factor was proposed for correcting the yield stress of the stress–strain relationship. It was confirmed that a practical estimation of the J-integral under biaxial loading can be

obtained by using the corrected stress–strain relationship and the reference stress solution for uniaxial loading. Additionally, it was confirmed that when α is between 0 and 1.0, a conservative estimation of the J-integral can be obtained by considering only the stress perpendicular to the crack plane and using the reference stress solution for uniaxial loading.

- (4) A multiaxial correction factor was modified for application to triaxial loading conditions. As a result of a comparison with the FEA results, it was confirmed that a practical estimation of the J-integral under triaxial loading can be obtained.

REFERENCES

- Aoki, T., Hattori, S., Anzai, H. and Sumimoto, H. (2005). “Stress Corrosion Cracking in Ni-base Alloy Used for a Long Time in a BWR.” *Maintenology*, Vol. 4, No. 1, 34-41.
- Bamford, W. and Hall, J. (2003). “A Review of Alloy 600 Cracking in Operating Nuclear Plants: Historical Experience and Future Trends.” *11th International Conference on Environmental Degradation of Materials in Nuclear Systems – Water Reactors*; 1071-1081. Stevenson, WA, August 10-14.
- Bjurman, M., Jädnäs, D., Kese, K., Jenssen, A., Chen, J., Cocco, M. and Johansson, H. (2017). “Root Cause Analysis of Cracking in Alloy 182 BWR Core Shroud Support Leg Crack.” *18th International Conference on Environmental Degradation of Materials in Nuclear Power Systems – Water Reactors*: 819-829. Portland, OR, August 13-17.
- Gustin, H. L., Cipolla, R. C., Xu, S. X. and Scarth, D. A. (2012). “Alternative Acceptance Criteria for Flaws in Ferritic Steel Components Operating in the Upper Shelf Temperature Range.” *Proceedings of the ASME 2022 Pressure Vessels & Piping Conference*, PVP2012-78190.
- Hayashi, T. et al. (2021). “Study on Fracture Behavior and Assessment for Dissimilar Metal Weld of Low Alloy Steel and Ni-base Alloy Weld Using a BWR Reactor Pressure Vessel Material,” *Proceedings of the ASME 2021 Pressure Vessels & Piping Conference*, PVP2021-61467.
- Lei, Y. (2004). “J-integral and limit load analysis of semi-elliptical surface cracks in plates under bending,” *International Journal of Pressure Vessels and Piping*, Vol. 81, 31-41.
- Matsunaga, T. and Matsunaga, K. (2003). “Stress Corrosion Cracking of CRD Stub Tube Joint and Repair at Hamaoka Unit 1.” *11th International Conference on Nuclear Engineering*, ICONE-36056.
- Miura, N. et al. (2000). “Systematization of simplified J-integral evaluation method for flaw evaluation at high temperature,” *Journal of Society of Material Science Japan*, Vol. 49, No. 8, 845-850 (in Japanese).
- Newman, J. C. and Raju, I. S. (1981). “An empirical stress-intensity factor equation for the surface crack,” *Engineering Fracture Mechanics*, Vol. 15, 185-192.
- Nuclear Regulatory Commission (NRC). (2017). “Limerick Generating Station, Unit 2 – Relief Request 14R-17, Associated with the Alternate Repair of a 2-inch Instrument Line Nozzle at Penetration N-16D on the Reactor Pressure Vessel (CAC NO. MF9702),” ADAMS Accession No: ML17208A090, August 14.
- Sattari-Far, I. (1994). “Finite element analysis of limit loads for surface cracks in plates,” *International Journal of Pressure Vessels and Piping*, Vol. 57, 237-243.
- Takanashi, M., Itatani, M., Nakane, M., Hojo, K., Takahashi, Y. and Okadaet, H. (2023). “Development of guideline for crack growth analysis method by reference stress – Activities of FDF-II Subcommittee, Atomic Energy Research Committee of JWES,” *14th International Conference on the Integrity of Nuclear Components*.